Spectroscopic Characterization of Polymer Adsorption at the Air–Solution Interface

Y. Ren,[‡] M. S. Shoichet, T. J. McCarthy, H. D. Stidham,[†] and S. L. Hsu[*]

Polymer Science and Engineering Department and the Materials Research Science and Engineering Center, University of Massachusetts, Amherst, Massachusetts 01003

Received July 12, 1994[⊛]

ABSTRACT: Infrared reflectance spectroscopy is used to investigate surface structure at the air–water interface for monomolecular layers of a semifluorinated alcohol, $CF_3(CF_2)_9(CH_2)_2OH$, and for water-soluble polymers of poly(ethylene oxide) samples end-capped with fluorinated hydrocarbon chains. In all cases, the fluorinated chain is highly ordered and oriented with the chain axis normal to the air–water surface. The highly ordered structure extends into the poly(ethylene oxide) backbone of the end-capped polymer chains. Reflectance intensities of the CF_2 stretching vibrations of the water-soluble polymers provide a direct measure of the surface concentration as a function of the bulk concentration and show that the Langmuir adsorption isotherm is strictly obeyed in the concentration range studied. There is no evidence of multiple layering at the surface. The Langmuir adsorption constant K was found to be 1.5×10^7 cm^3/mol for poly(ethylene oxide) end-capped with $CO(CF_2)_8CF_3$.

Introduction

Infrared reflectance spectroscopy is a useful method for the structural investigation of thin films cast on solid or liquid substrates. The incident beam is directly reflected from metallic substrates, and the transmitted beam is attenuated in regions of substrate absorption for other materials. The reflected beam interacts with molecules situated at the surface of partially transmitting materials. The resulting reflectance spectra are functions of polarization and incidence angle of the incident beam and provide a quantitative measure of the surface concentration and an indirect measure of the structure and orientation of molecules in the surface layer.

In the early work conducted at air–water interfaces in this laboratory, the reflectance spectra of several apparently insoluble long fluorinated and hydrogenated alcohols were investigated in both s and p polarization at incidence angles ranging from near grazing ($\sim80°$) to near normal ($\sim0°$). In this investigation, it became clear that the method used for spreading an apparently insoluble material on a liquid substrate surface (by dissolving it at an appropriate concentration in a solvent insoluble in the liquid substrate and spreading the solution on the substrate) did not rapidly produce an equilibrium. The surface concentration is governed by the Gibbs adsorption isotherm relating the bulk to the surface concentration and varied with time as the apparently insoluble materials very slowly dissolved. Although the films spread rapidly on the surface of the water and equilibrium was rapidly achieved in the film as initially cast, the reflectance spectrum displayed a time dependence, and even vanished entirely in unfavorable cases. To avoid these difficulties, the focus of the investigation was altered to films composed of polymeric materials clearly soluble in the liquid substrate, water. Results are reported here for one of these alcohols, $CF_3(CF_2)_9(CH_2)_2OH$, to illustrate the principles underlying the estimate of orientation for the relatively rigid end group.

* To whom correspondence should be sent.
† Department of Chemistry.
‡ Department of Physics.

The properties of polymers in constrained geometries are often much different from those in the bulk phase.[1] The microstructure of polymers at the air–water interface is not well investigated and deserves further study. Ellipsometry,[2,3] surface pressure,[4] surface light scattering,[5] and neutron scattering[6] have been used recently to study monolayers of polymers at the air–water interface. Poly(ethylene oxide) was studied by ellipsometry,[2] and the film thickness measured by this method suggests that poly(ethylene oxide) assumes flattened conformations in the surface film. Radioisotope labeling has been used to assess the small amount of adsorbed matter, typically of the order of $10^{-7}–10^{-6}$ g cm^{-2}, but the method provides no structural information.[7]

There have been extensive studies reported for the use of external reflection infrared spectroscopy applied to thin polymer films cast on a metal substrate.[8–10] In addition to preliminary studies in this laboratory, insoluble monolayers at the air–water interface have been studied by Buontempo,[11] Fina,[12] Gericke,[13] and Dluhy.[14] No polymers were involved in any of these studies, and there appear to be no reports of infrared reflectance spectra of polymers at air–solution interfaces. The polymeric solutes chosen for this study were pure poly(ethylene oxide) and poly(ethylene oxide) of two molecular weights end-capped with perfluorinated alkyl groups. Water is a good solvent for all of these materials.

Nearly monodisperse samples of poly(ethylene oxide) [PEO], poly(ethylene oxide) with molecular weight 5000 end-capped with $CO(CF_2)_8CF_3$ [PEO(5K)–$CO(CF_2)_8CF_3$] or $CO(CF_2)_2CF_3$ [PEO(5K)–$CO(CF_2)_2CF_3$], and poly(ethylene oxide) with molecular weight 50000 end-capped with $CO(CF_2)_8CF_3$ [PEO(50K)–$CO(CF_2)_8CF_3$] were synthesized for use in this work. The perfluorinated end groups are hydrophobic and when the end-capped polymers are dissolved in water, the end groups are expected to accumulate preferentially at the air–water interface. The ellipsometric results suggest that the poly(ethylene oxide) chain may be in a flattened random coil conformation. The structure and conformation of the end-capped polymer in the surface layer are, however, open to experimental investigation. The infrared reflectance spectra reported below strongly suggest a highly ordered structure for the end group and

for the poly(ethylene oxide) backbone segments to which the end groups are attached. Penetration of the incident polarized infrared beam into the solution is strongly attenuated, and no structural information is available for poly(ethylene oxide) segments that are more deeply buried in the first surface layer. This is because there are no other interfaces below the surface layer to reflect the incident beam. In this specific case, the sampling depth is of the order of the thickness of the surface layer, several hundred angstroms.

The formation of the surface layer may be viewed as a process of adsorption from solution, and the Langmuir adsorption isotherm is appropriate to treat the case of monolayer adsorption. Departures of the observed adsorption isotherm from the Langmuir result would reflect an alternative layering. The results reported here for end-capped poly(ethylene oxide) show nearly exact agreement with the Langmuir isotherm and display no evidence of curvature suggesting a multiple layering more appropriately described by a 2- or 3-layer or Brunauer–Emmett–Teller adsorption isotherm.[15,16]

Experimental Section

$CF_3(CF_2)_9(CH_2)_2OH$ (PCR Inc., Gainesville, FL) was used as received to spread monolayer films on water from n-hexane solution. Solutions were prepared with concentrations to produce films with a calculated area per molecule. Microsyringes used to measure volumes of n-hexane solution were purged with solvent tens of times before each spread. All experiments were repeated several times to confirm reproducibility. Films were typically allowed to equilibrate for at least 10 min after the initial spread. The water used to charge the trough in which the film was spread was purified with a Millipore ultrapure water system.

Poly(ethylene oxide) was prepared by anionic ring-opening polymerization of ethylene oxide using potassium triethylene glycol monomethyl ether as the initiator in THF solution. THF was distilled from sodium benzophenone dianion; ethylene oxide was distilled from calcium hydride. Polymerization was allowed to proceed at 40 °C for ~40 h under nitrogen. Polymerization was terminated with degassed methanol, and poly(ethylene oxide) was isolated by precipitation in hexane. Samples were redissolved in THF and reprecipitated in hexane twice. End-capping reactions were carried out overnight by reacting poly(ethylene glycol) samples with heptafluorobutyryl chloride or nonadecafluorodecanoyl chloride in THF with pyridine catalysis at 40 °C. Polymer samples were isolated and purified as described for poly(ethylene oxide). Elemental analysis indicated 64–96% yields for the esterification reactions. The molecular weights of the polymers were measured by gel permeation chromatography against poly(ethylene oxide) standards. The $PEO(5K)-CO(CF_2)_8CF_3$ or $PEO(50K)-CO(CF_2)_8CF_3$ samples had molecular weights of 5 and 50 kg/mol, respectively, while $PEO(5K)-CO(CF_2)_2CF_3$ has a molecular weight of about 5 kg/mol. The polydispersity indices of these samples ranged from 1.07 to 1.17.

$PEO(5K)-CO(CF_2)_8CF_3$, $PEO(50K)-CO(CF_2)_8CF_3$, and $PEO(5K)-CO(CF_2)_2CF_3$ were dissolved in clean water at different concentrations below or above 1.0 mg/mL several days before the experiments. All three polymers are completely water soluble and give clear solutions. In contrast to the insoluble monolayer experiments, no spreading was conducted. The experiments are done as follows. A certain volume of clean water was transferred into the trough and the FTIR reflectance background was obtained. Exactly the same volume of polymer solution was used to collect the sample spectrum. The ratioed spectrum was further transformed to absorbance units.

Transmission spectra of KBr pellets of polymers were obtained with an IBM 38 spectrometer equipped with a DTGS detector. All transmission spectra were collected by coaddition of 128 scans at 2 cm^{-1} resolution.
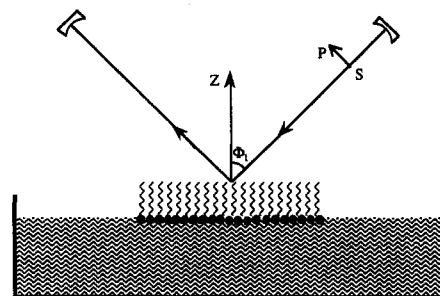

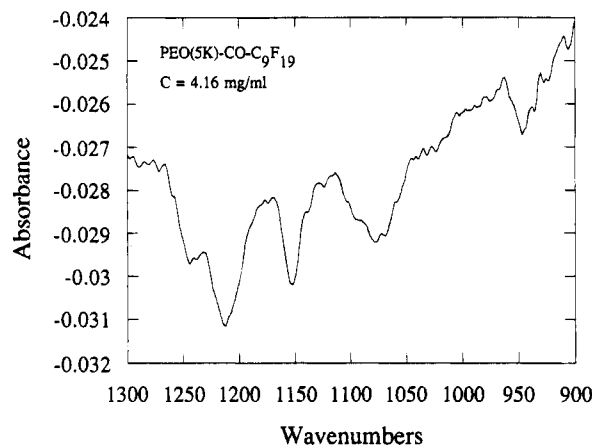**Figure 1.** Schematic illustration of the experimental setup.

Figure 2. s polarization reflectance spectrum of PEO(5K)–CO(CF_2)_8CF_3 at solution concentration equal to 4.16 mg/mL.

A schematic illustration of the reflectance experiment is shown in Figure 1. Reflectance spectra were obtained with a Perkin-Elmer 2000 FTIR spectrometer equipped with a narrow-band MCT detector using an external reflection cell purchased from Graesby Specac in Waterbury, CT. The angle of incidence may be varied from 0 to nearly 90° measured relative to the surface normal. All experiments were conducted at 30° incidence angle. The cell is equipped with a removable Teflon trough. Since the molecules are on the surface of water, no attempts were made to purge the sample compartment. Water evaporation presents a problem in mismatch between the sample and background spectrum. The resulting absorbance spectrum can be greatly distorted and the band position and intensity will no longer be accurate. A wavelike baseline in the spectrum occurs on mismatch. For this reason, the time interval between the sample and background spectrum is set to be within 15 min. The polarizer was set directly above the water surface to ensure the optimum polarizing effect. All spectra were collected at 4 cm^{-1} resolution. In all cases 256 scans were coadded to obtain acceptable signal to noise ratio. The s polarization infrared spectra of solutions of PEO(5K)–CO(CF_2)_8CF_3 and PEO(50K)–CO(CF_2)_8-CF_3 are shown in Figures 2 and 3. These represent the typical spectra obtained.

The surface tension vs bulk solution concentration curve was measured by using a KSV 5000 Langmuir–Blodgett trough from KSV Instruments (Monroe, CT). The temperature of the trough is not controlled. The room temperture of the air-conditioned laboratory in which the trough was installed was routinely kept at 24 ± 1 °C. The surface tension of each solution was measured by the Welhelmy method. The surface pressure was measured for PEO(50K)–CO(CF_2)_8CF_3 solutions with different concentration.

Method Section

The number of perfluorinated end caps of the PEO–R polymers at an air–solution surface was determined by comparing the reflectance spectrum with that of a densely populated film of the insoluble alcohol $CF_3(CF_2)_9(CH_2)_2OH$ cast on water. The treatment presented by Flournoy and Schaffers for attenuated
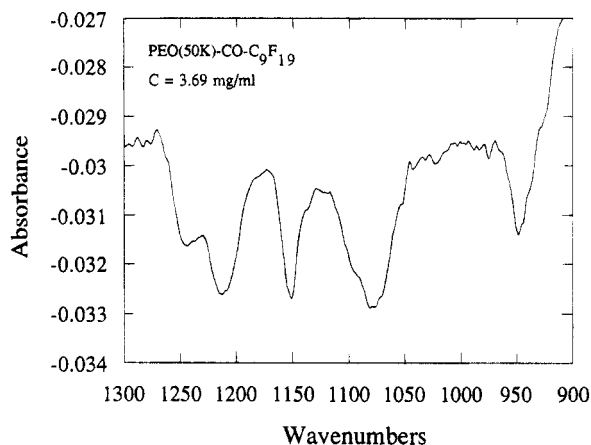
Figure 3. s polarization reflectance spectrum of PEO(50K)–CO(CF$_2$)$_8$CF$_3$ at solution concentration equal to 3.69 mg/mL.

total reflection from surfaces of absorbing anisotropic films cast on isotropic nonabsorbing substrates was modified to describe the geometry given in Figure 1.[17] This geometry differs from that considered by Flournoy and Schaffers in two ways. First, the incident light is propagated in air rather than in an isotropic nonabsorbing crystalline medium. Second, the isotropic medium (water) in Figure 1 on which the film is cast is absorbing rather than nonabsorbing, and the refractive index is accordingly complex rather than real. The analysis is otherwise very similar to that given by Born and Wolf, the critical equations being that of Fresnel[18] and the complex form of Snell's law relating complex refractive indices and propagation direction angels in layered absorbing materials.

The complex refractive indices in the absorbing anisotropic film are unknown but may be written $\hat{n}_{\alpha\alpha} = n_{\alpha\alpha} + ik_{\alpha\alpha}$ ($\alpha = x, y, z$), where the z axis is taken normal to the surface, the x axis is out of the plane of incidence, and the y axis is in it. For any vibration of the molecules in the film, these refractive indices are related to the transition dipole orientation angles (Θ,ϕ) and the dipole strength $K(\omega)$ by

$$k_{xx} = K(\omega)\langle\sin^2\Theta\cos^2\phi\rangle$$

$$k_{yy} = K(\omega)\langle\sin^2\Theta\sin^2\phi\rangle$$

$$k_{zz} = K(\omega)\langle\cos^2\Theta\rangle \tag{1}$$

where $K(\omega)$ is proportional to the number of chemical units in the film and to the square of the dipole moment change associated with the vibration. In the absence of the incident light, there is nothing to distinguish the x from the y direction in the film, and then $n_{xx} = n_{yy} = n_\perp$. However, due to film orientation effects n_{zz} may be quite different. The absence of preferential orientation in the plane of the film allows classical averaging to be used and $\langle\cos^2\phi\rangle = \langle\sin^2\phi\rangle = 1/2$. This allows writing

$$k_{xx} = k_{yy} = K_\perp = K(\omega)\frac{\langle\sin^2\Theta\rangle}{2}$$

$$k_{zz} = K_\parallel = K(\omega)\langle\cos^2\Theta\rangle \tag{2}$$

The complex reflectivity r follows from Fresnel's equation as described by Flournoy and Schaffers.[17] The real reflectivity R is the squared modulus of the complex reflectivity r, and the reflectance A relative to that of

water alone is given in either s or p polarization by

$$A = -\log(R/R_0) \tag{3}$$

where R_0 is the real reflectivity of the absorbing isotropic substrate with film removed.

Some preliminaries are necessary before the main computation can be performed. The fluorinated insoluble alcohol CF$_3$(CF$_2$)$_9$(CH$_2$)$_2$OH has two broad intense bands near 1151 and 1207 cm^{-1}, with a weaker one at 1232 cm^{-1} and even weaker progression bands at 1113, 1088, and 1065 cm^{-1}.[19,20] The 1151 and 1207 cm^{-1} bands are respectively assigned as the symmetric and antisymmetric CF$_2$ stretches.[19-25] The 1151 cm^{-1} band is known to be perpendicularly polarized, but the state of polarization of the 1207 cm^{-1} band is not clearly described by earlier workers. Recent work on the infrared dichroic ratio of coextruded poly(vinylidene difluoride-co-ethylene trifluoride) [P(VDF–TrFE)] copolymer at a draw ratio of 6.0 shows the dipole moment changes for both CF$_2$ stretching bands are perpendicular to the main chain direction.[26]

The reflectance experiments for the water-insoluble alcohol CF$_3$(CF$_2$)$_9$(CH$_2$)$_2$OH were conducted at a constant surface concentration selected to give an average surface area per molecule of 27.5 Å^2/molecule. This value was selected to be slightly greater than the cross-sectional area of 25 Å^2/molecule found by earlier workers for the fully packed state.[27,28] In such a film, it is very unlikely that any chains lie on the water surface, though it is possible in principle for the CF$_2$ helical axis to be inclined at some angle Θ_{chain} to the surface normal.

Quantitative analysis for the polymer films requires values of $K(\omega)$ and Θ for each infrared band used. These were transferred from the CF$_2$ stretching vibrations of the fluorinated alcohol by obtaining relative reflectance data for the film above as a function of incidence angle in both s and p polarizations. A least squares fit of these data was made to relative reflectance curves calculated for a series of values of $K(\omega)$ and Θ for the complex refractive indices of water appropriate to the band. For 1151 cm^{-1} band, n(water) = 1.269 + i0.0383, and for 1207 cm^{-1} band n(water) = 1.283 + i0.0361.[29] For the 1151 cm^{-1} band, least squares $K(\omega)$ and Θ were found to be 3.03 and 90°, while for the 1207 cm^{-1} band the results were 2.22 and 90°. Since the direction cosines must obey the relation

$$\cos^2\Theta_{chain} + \cos^2\Theta_{1151} + \cos^2\Theta_{1207} = 1 \tag{4}$$

the chain orientation angle in the film of fluorinated alcohol must be 0°, measured with respect to the surface normal. Thus, all the transition moments of the CF$_2$ stretching vibrations of the fluorinated alcohol are parallel to the surface plane, and all of the perfluorinated helices are oriented with the main axes exactly perpendicular to the surface. Further details of these calculations are described elsewhere.[30]

Since the fluorinated part of CF$_3$(CF$_2$)$_9$(CH$_2$)$_2$OH is so strongly hydrophobic that it is aligned perpendicular to the water surface, the fluorinated part of the end-capped polymers PEO–R were assumed to be similarly aligned at all concentrations. Evidence supporting this hypothesis is presented in Figures 4 and 5. In Figure 4, the s-polarized reflectance spectra for films of PEO, PEO–CO(CF$_2$)$_8$CF$_3$, and PEO(5K)–R are presented in the CF$_2$ stretching region, and in Figure 5, the transmission spectrum of CF$_3$(CF$_2$)$_9$(CH$_2$)$_2$OH is shown in the crystalline and molten states. The bandwidths of the CF$_2$ stretching vibrations are much narrower in the
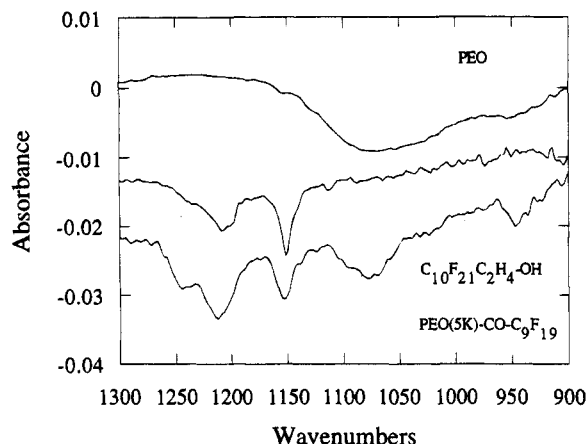
Figure 4. s polarization reflectance spectra of PEO, $F(CF_2)_{10}(CH_2)_2$ OH and PEO(5K)–CO(CF$_2$)$_8$CF$_3$.
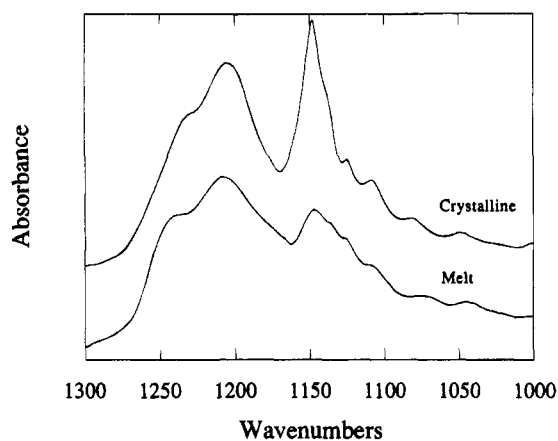

Figure 5. Transmission spectra of $CF_3(CF_2)_9(CH_2)_2OH$ in the crystalline and melt states.

crystalline state than in the melt, reflecting the distribution of conformational states each with somewhat different CF_2 stretching frequencies present in the melt. Similarly, the narrow bandwidths found for the CF_2 stretching vibrations in the reflectance spectra of Figure 4 strongly suggest a lack of conformational variety at the surface in both the alcohol and the polymer.

When Θ is set equal to 90° for the polymer, the relative reflectance at constant incidence angle is proportional both to the number of absorbing molecules in the surface and to the transition dipole strength $K(\omega)$, which is itself proportional to the number of CF_2 groups in the perfluorinated chain. The model calculation proved that the s polarization reflectance is linearly proportional to absorption constant K, as shown in Figure 6. Thus, the number of PEO–R ends at the surface can be determined from the relative reflectance by using $K(\omega)$ for the fluorinated alcohol modified to account for the difference in the number of CF_2 groups and to account for the number of fluorinated alcohol molecules in the surface at the surface coverage used. Let N be the number of PEO–R polymer molecules at the air–solution interface, N_0 be the number of fluorinated alcohol molecules present in the thin film of insoluble alcohol cast on water, As_0 be the s-polarized relative reflectance of the fluorinated alcohol, and As be the s-polarized relative reflectance of a polymer solution of concentration c obtained at the same incidence angle. The relation that allows N to be determined is
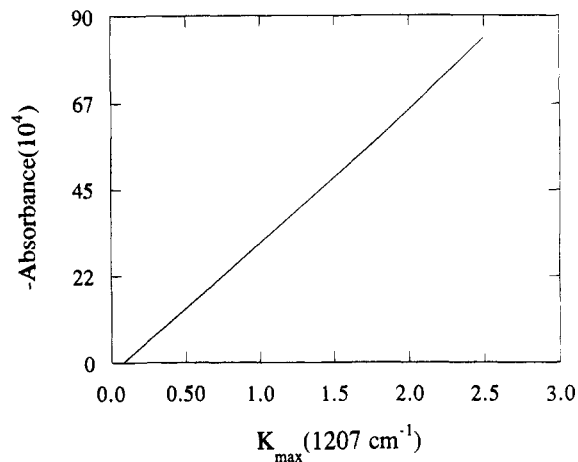
Figure 6. Model calculation of s polarization reflectance As as a function of absorptivity K for a model monolayer at the air–water interface. Film thickness is 14.57 Å, and $n_\perp$ and $n_\parallel$ are 1.3 and 1.6. Band frequency is at 1207 cm^{-1}, and Θ is set to be 90°. The other parameters are described in the text.
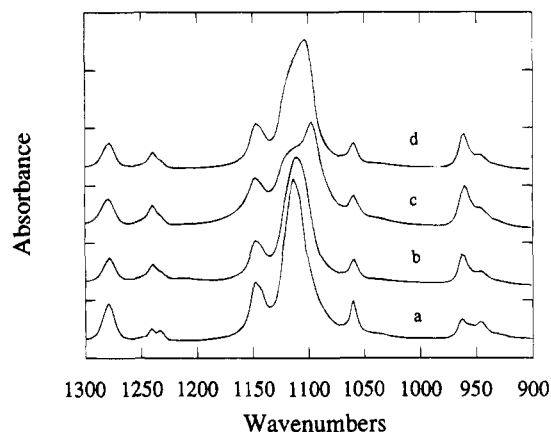

Figure 7. Bulk transmission spectra of PEO and PEO-R samples: (a) PEO; (b) PEO(5K)–CO(CF$_2$)$_8$CF$_3$; (c) PEO(50K)–CO(CF$_2$)$_8$CF$_3$; (d) PEO(5K)–CO(CF$_2$)$_2$CF$_3$.

$$N = \frac{As}{0.9As_0}N_0 \tag{5}$$

where 0.9 accommodates the 1 CF_2 group difference between the alcohol and the end cap. Since the surface area per molecule selected for the alcohol is 27.5 Å^2/molecule, the number of alcohol molecules at the interface N_0 is the area of the trough divided by 27.5, or 7.5×10^{15} molecules. The 1207 cm^{-1} band was used to construct the isotherm, and for this band As_0 was -73.6×10^{-4}. The s-polarized relative reflectance As was measured for PEO-CO(CF$_2$)$_8$CF$_3$ solutions of various bulk concentrations c and the results used to provide a measure of N as a function of c.

Results and Discussion

The transmission infrared spectrum of each of the polymer samples is displayed from 900 to 1300 cm^{-1} in Figure 7. It is particularly noteworthy that the antisymmetric CF_2 stretching band expected at 1207 cm^{-1} does not appear for any of the end-capped PEO–R polymers. All of these spectra were obtained under as nearly identical conditions as possible. Presumably, the fluorinated fraction of the end-capped polymers is small enough that the intensities are too low to be easily seen in a transmission experiment under the conditions used. In contrast, the antisymmetric CF_2 stretching vibration dominates the reflectance spectra for end-capped poly-
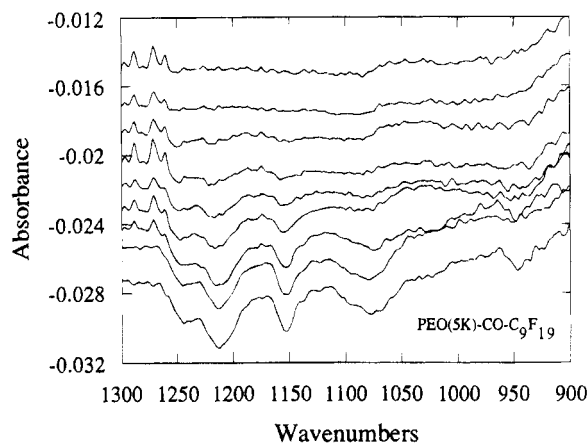
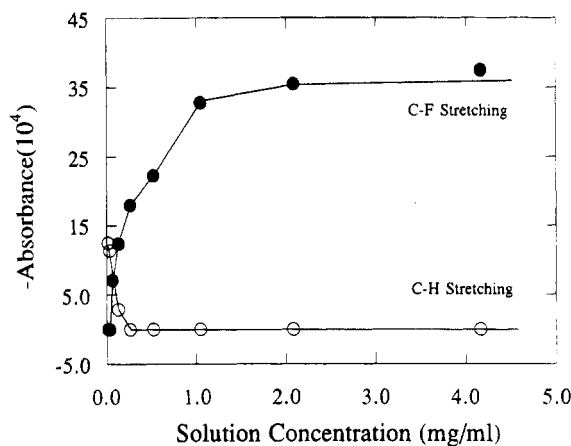**Figure 8.** Reflectance spectra of PEO(5K)−CO(CF$_2$)$_8$CF$_3$ as a function of bulk solution concentration.

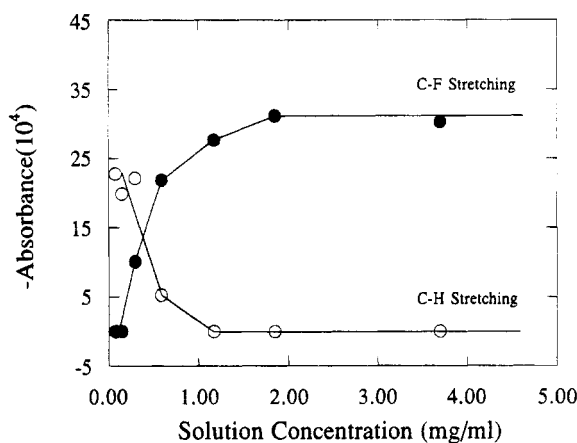**Figure 9.** s polarization reflectance of C−F and C−H stretching bands of PEO(5K)−CO(CF$_2$)$_8$CF$_3$.

Figure 10. s polarization reflectance of C−F and C−H stretching bands of PEO(50K)−CO(CF$_2$)$_8$CF$_3$.

mers at the surface, and the intensity ratio of the CF$_2$ to CH$_2$ stretching bands is inverted.

Reflectance spectra for PEO(5K)−CO(CF$_2$)$_8$CF$_3$ are shown in the 900−1300 cm^{-1} region as a function of solution concentration in Figure 8. Similar spectra were observed for PEO(50K)−CO(CF$_2$)$_8$CF$_3$. In Figures 9 and 10, the intensity of the relative reflectance of the antisymmetric CF$_2$ stretching vibration near 1213 cm^{-1} increases with solution concentration but reaches a plateau at larger concentrations. These intensities were used to calculate the number of perfluorinated end groups at the air−solution interface.

Interestingly, either no or very weak CF stretching bands were observed for all concentrations of PEO(5K)−

CO(CF$_2$)$_2$CF$_3$. It was found in an earlier study of partially fluorinated surface-active agents at the air−water interface that there is a monolayer stability transition that occurs between 8 and 10 CF$_2$ groups in the surface-active molecules.[31] No features were observed in the 1000−1300 cm^{-1} region in the reflectance spectrum of a film of CF$_3$(CF$_2$)$_7$(CH$_2$)$_2$OH spread on water, but strong bands were found in the reflectance spectrum of a film of the longer molecule CF$_3$-(CF$_2$)$_9$(CH$_2$)$_2$OH spread on water. However, intense CH$_2$ stretching vibrations were found in both reflectance spectra. Evidently, short CF$_2$ chains do not form helices well and cannot organize at the interface but pack randomly. Only longer chains are capable of forming helices and displaying the orientation effects found for CF$_3$(CF$_2$)$_9$(CH$_2$)$_2$OH and the two PEO−R polymers end-capped with the longer CF$_2$ chains.

The C−O−C stretching and CH$_2$ stretching and rocking regions give information about the structure of the PEO chain near the surface. The relative reflectance intensity of one of the CH stretching vibrations is plotted as a function of solution concentration for both PEO(5K)−CO(CF$_2$)$_8$CF$_3$ and PEO(50K)−CO(CF$_2$)$_8$CF$_3$ in Figures 9 and 10, superposed on the data for the antisymmetric CF$_2$ stretch. The opposing trends of intensity can be explained as an optical phenomenon. The depth of penetration of the incident infrared beam into the solution depends on the concentration profile of the polymer solution in the surface region. In concentrated solution, the surface layer is densely packed with perfluorinated end groups. The infrared beam mostly reflects from these, and very little light reaches the lower parts containing the hydrogenous PEO fraction of the end-capped polymer. In dilute solution, most of the light reflects from the water surface. Since water has a different complex refractive index than densely packed perfluorinated end groups, the depth of penetration is different. Relatively little light reflects from the smaller number of perfluorinated end groups, and the depth of penetration is sufficient to reach the very much larger number of CH$_2$ groups in random coils of PEO associated with the end groups. As a result, the reflectance spectrum is much stronger in the CH stretching region for dilute solutions of end-capped polymer than it is for concentrated solutions. The opposing trends of reflectance intensity for CH and CF stretching are supporting evidence for accumulation of perfluorinated end groups in the surface. Furthermore, the reflectance spectrum of PEO−CO(CF$_2$)$_8$CF$_3$ shows very weak CF stretching bands and intense CH stretching bands.

The s-polarized reflectance spectra of solutions PEO and PEO(50K)−CO(CF$_2$)$_8$CF$_3$ shown in Figure 4 provide evidence of surface ordering in the hydrogenous chain attached to the perfluorinated end caps. Matsui[32] and Matsuura[33] assigned bands near 1079 and 949 cm^{-1} in bulk poly(ethylene oxide) to mixed CO stretching, CF$_2$ rocking, and CC stretching and to CH$_2$ rocking mixed with CO stretching, respectively. These bands are observed as sharp features in the reflectance spectrum of PEO(5K)−CO(CF$_2$)$_8$CF$_3$ solution, but only as very broad features in the reflectance spectrum of PEO solution. The breadth of the PEO solution reflectance spectrum strongly suggests a wide distribution of conformers in molecules near the surface consistent with a surface-modified random coil, while the much sharper features in the reflectance spectrum of PEO(50K)−CO-(CF$_2$)$_8$CF$_3$ solution suggest a smaller distribution of conformations in the part of the PEO chain that can be accessed in the penetration depth of the incident

infrared light. Evidently, the extreme hydrophobicity of the perfluorinated end caps introduces order not only in the perfluorinated layer but also in the PEO backbone units attached to the end caps.

In a system of polymer dissolved in a good solvent, polymer molecules will continually approach and leave the air−solution interface. An equilibrium will be reached with an exact balance between the rate of approach and departure. If the random coils of PEO are nonpenetrating, the maximum number of surface sites is essentially determined by the cross-sectional area of PEO coils at the surface of a saturated solution. In these circumstances, the appearance of a number of end-capped PEO molecules at the surface can be treated as an adsorption problem. If the adsorption occurred in two layers, with the second layer deposited only on the sites occupied by molecules in the first layer, the appropriate single-site grand partition function is

$$\zeta = 1 + q_1\lambda + q_1q_2\lambda^2 \qquad (6)$$

where q_1 is the partition function for a molecule in the first layer, q_2 is the partition function for a molecule in the second layer, and λ is the activity.[16] The mean fractional occupation Θ is

$$\Theta = \left(\frac{\partial \ln \zeta}{\partial \ln \lambda}\right)_{T,b} \qquad (7)$$

where b is the maximum number of sites for adsorption and T is the temperature. The adsorption isotherm is immediate

$$\Theta = \frac{q_1 + 2q_1q_2\lambda^2}{1 + q_1\lambda + q_1q_2\lambda^2} \qquad (8)$$

Take $K = q_1/q_2$ and set $q_2\lambda = c$. Then

$$\Theta = \frac{Kc(1 + 2c)}{1 + Kc(1 + c)} \qquad (9)$$

which may be rearranged to

$$\Theta = \frac{Kc(1 - 3c^2 + 2c^3)}{(1 - c)(1 - c + Kc - Kc^3)} \qquad (10)$$

When c is small enough, quadratic and higher powers may be neglected and the relative coverage may be written approximately as

$$\Theta = \frac{Kc}{(1 - c)(1 - c + Kc)} \qquad (11)$$

which is the Brunauer−Emmett−Teller adsorption isotherm. If additionally c is small compared with unity while K is large enough, the relative coverage is approximately

$$\Theta = \frac{Kc}{1 + Kc} \qquad (12)$$

which is the Langmuir adsorption isotherm. Since Θ is the relative coverage, it may be written as N/b, where N is the number of perfluorinated end caps at the surface. Then a plot of N measured by infrared reflectance against the bulk concentration should obey the equation
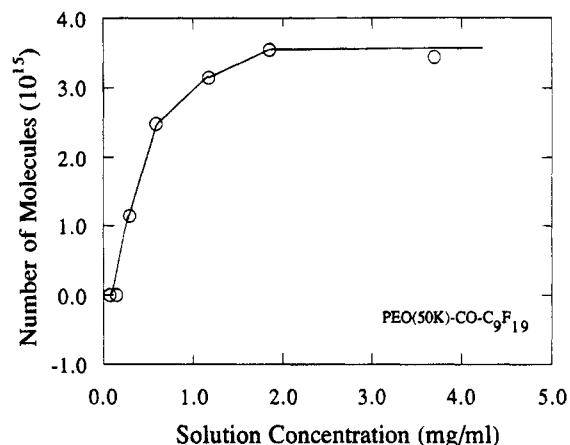
$$N = \frac{bKc}{1 + Kc} \qquad (13)$$

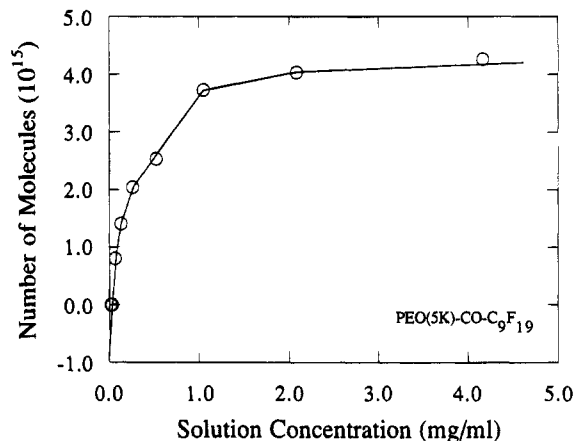**Figure 11.** Number of polymer ends at the air−solution interface as a function of bulk solution concentration: PEO(50K)−CO(CF$_2$)$_8$CF$_3$.

Figure 12. Number of polymer ends at the air−solution interface as a function of bulk solution concentration: PEO(5K)−CO(CF$_2$)$_8$CF$_3$.
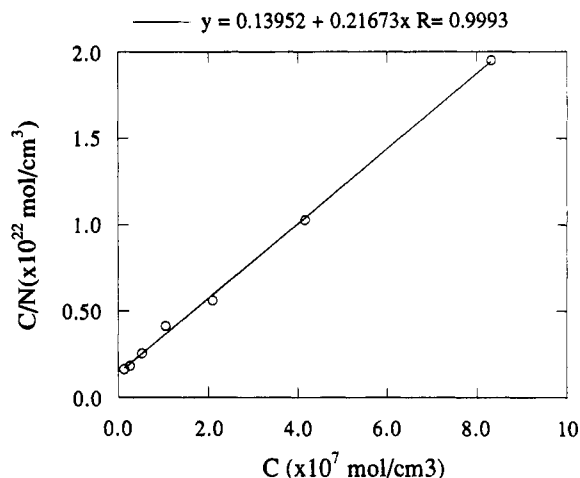

Figure 13. Langmuir plot of eq 1: PEO(5K)−CO(CF$_2$)$_8$CF$_3$.

Shown in Figures 11 and 12, the data correspond within experimental error with this equation. Furthermore, the number of chain ends of PEO(5K)−CO(CF$_2$)$_8$CF$_3$ is larger than the number for solutions of PEO(50K)−CO(CF$_2$)$_8$CF$_3$ at the same concentration, showing that b is determined by the size of the PEO random coils at the interface.

The Langmuir equation is often rewritten as

$$\frac{c}{N} = \frac{1}{bK} + \frac{1}{b}c \qquad (14)$$

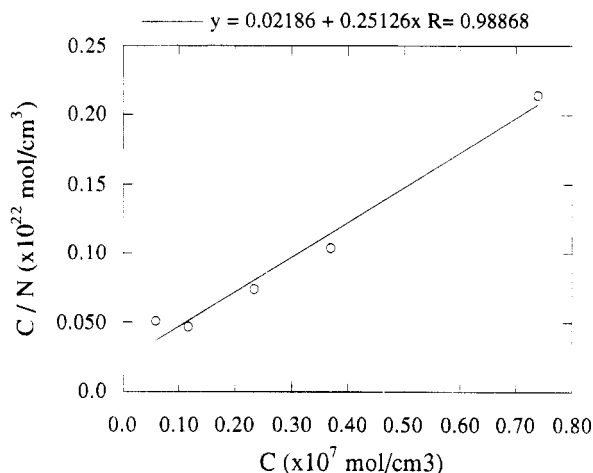Since b and K are constants at constant temperature, a
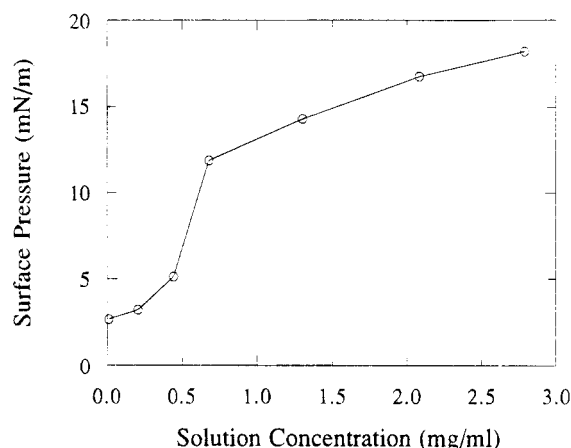
Figure 14. Langmuir plot of eq 1: $PEO(50K)-CO(CF_2)_8CF_3$.

Figure 15. Surface tension isotherm of $PEO(50K)-CO(CF_2)_8-CF_3$.

Table 1. Results of Langmuir Adsorption Isotherm Plot

	$PEO(5K)-$ $CO(CF_2)_8CF_3$	$PEO(50K)-$ $CO(CF_2)_8CF_3$
equilibrium adsorption constant K (cm^3/mol)	1.553×10^7	1.149×10^8
max no. of sites b	4.614×10^{15}	3.980×10^{15}

plot of c/N against c should give a straight line of slope b^{-1} and intercept $(bK)^{-1}$. Figures 13 and 14 show no evidence of curvature and give excellent agreement with the linearized Langmuir equation. Further, the reciprocal slope is equal to b, the maximum number of sites, and the ratio of these two slopes stands in the ratio of the average cross-sectional area of the 5K and 50K polymers in the surface layer of a saturated solution. The ratio of the slope is equal to 0.86. Thus the higher molecular weight polymer gives a larger cross-sectional area. Table 1 summarizes these results.

To confirm the results, we have also done surface tension measurements. The result shown in Figure 15 clearly suggests that the surface tension of more concentrated polymer solution is further lowered by the polymers adsorbed at the interface. Particularly, the surface tension approaches to a plateau when the bulk concentration exceeds 1.0 mg/mL. This result agrees well with the results obtained from spectroscopic measurements.

Conclusion

Infrared reflectance spectra obtained from the air–solution interface of aqueous PEO and PEO—R solutions strongly suggest that the hydrophobic end groups are highly ordered and that all of the perfluorinated helices are oriented with the helix axis normal to the surface. The end-capped polymers also appear more ordered at the surface of these solutions than does the PEO homopolymer. The reflectance intensities are consistent with detection of a single layer and follow the Langmuir adsorption isotherm quantitatively.

References and Notes

(1) Sanchez, I. C., Ed.; *Physics of Polymer Surfaces and Interfaces*; Reed Publishing (USA) Inc.: Stoneham, 1992.

(2) Kawaguchi, M.; Tohyama, M.; Takahashi, A. *Langmuir* **1988**, *4*, 407–413.

(3) Sauer, B. B.; Yu, H.; Yazdanian, M.; Zografi, G.; Kim, M. W. *Macromolecules* **1989**, *22*, 2332–2337.

(4) Lu, J. R.; Marrocco, A.; Su, T. J.; Thoamas, R. K.; Penfold, J. *J. Colloid Interface Sci.* **1993**, *158*, 303.

(5) Yu, H. In *Physics of Polymer Surfaces and Interfaces*; Sanchez, I. C., Ed.; Reed Publishing (USA) Inc.: Stoneham, 1992; Chapter 12.

(6) Stamm, M. In *Physics of Polymer Surfaces and Interfaces*; Sanchez, I. C., Ed.; Reed Publishing (USA) Inc.: Stoneham, 1992; Chapter 8.

(7) Adamson, A. W. *Physical Chemistry of Surfaces*; John Wiley & Sons, Inc.: New York, 1990.

(8) Rabolt, J. F. In *Physics of Polymer Surfaces and Interfaces*; Sanchez, I. C., Ed.; Reed Publishing (USA) Inc.: Stoneham, 1992; Chapter 14.

(9) Nuzzo, R. G.; Dubois, L. H.; Allara, D. L. *J. Am. Chem. Soc.* **1990**, *112*, 558.

(10) Allara, D. L.; Nuzzo, R. G. *Langmuir* **1985**, *1*, 52.

(11) Buontempo, J. T.; Rice, S. A. *J. Chem. Phys.* **1993**, *98*, 583.

(12) Fina, L. J.; Tung, Y. *Appl. Spectrosc.* **1991**, *45*, 986.

(13) Gericke, A.; Michailov, A. V.; Huhnerfuss, H. *Vib. Spectrosc.* **1993**, *4*, 335.

(14) Dluhy, R. A. *J. Phys. Chem.* **1986**, *90*, 1373.

(15) Brunauer, S.; Emmett, P. H.; Teller, E. *J. Am. Chem. Soc.* **1938**, *60*, 309.

(16) Hill, T. L. *J. Chem. Phys.* **1946**, *14*, 263.

(17) Flournoy, P. A.; Schaffers, W. *J. Spectrochim. Acta* **1966**, *22*, 5.

(18) Born, M.; Wolf, E. *Principles of Optics*; Pergamon Press: London, 1959.

(19) Hsu, S. L.; Reynolds, N.; Bohan, S. P.; Strauss, H. L.; Snyder, R. G. *Macromolecules* **1990**, *23*, 4565.

(20) Rabolt, J. F.; Fanconi, B. *Macromolecules* **1978**, *11*, 740.

(21) Cho, H. G.; Strauss, H. L.; Snyder, R. G. *J. Phys. Chem.* **1992**, *96*, 5290.

(22) Masetti, G.; Cabassi, F.; Morelli, G.; Zerbi, G. *Macromolecules* **1973**, *6*, 700.

(23) Zerbi, G.; Sacchi, M. *Macromolecules* **1973**, *6*, 692.

(24) Naselli, C.; Swalen, J. D.; Rabolt, J. F. *J. Chem. Phys.* **1989**, *90*, 3855.

(25) Chidsey, C. E. D.; Loiacono, D. N. *Langmuir* **1990**, *6*, 682.

(26) Bakeev, K. A. Ph.D. Thesis, University of Massachusetts at Amherst, 1993.

(27) Piseri, L.; Powell, B. M.; Dolling, G. J. *J. Chem. Phys.* **1973**, *58*, 158.

(28) Bernett, M. K.; Zisman, W. A. *J. Phys. Chem.* **1963**, *67*, 1534.

(29) Downing, H. D.; Williams, D. *J. Geophys. Res.* **1975**, *80*, 1656.

(30) Ren, Y.; Meuse, C. W.; Stidham, H. D.; Hsu, S. L. *J. Phys. Chem.* **1994**, *98*, 8424.

(31) Meuse, C. W. Ph.D. Thesis, University of Massachusetts at Amherst, 1993.

(32) Matsui, Y.; Kubota, T. *J. Polym. Sci., Part A* **1965**, *3*, 2275–2288.

(33) Matsuura, H.; Miyazawa, T. *Spectrochim. Acta* **1973**, *29A*, 771–779.

MA9410290